

...

Matt Ellis

A dissertation submitted in partial fulfillment  
of the requirements for the degree of  
Doctor of Philosophy  
of  
University College London.

Department of Physics and Astronomy  
University College London

July 27, 2020

I, Matt Ellis, confirm that the work presented in this thesis is my own. Where information has been derived from other sources, I confirm that this has been indicated in the work.

# Abstract

My research is about stuff.

It begins with a study of some stuff, and then some other stuff and things.

There is a 300-word limit on your abstract.

# Acknowledgements

Acknowledge all the things!

# Contents

1	Introduction	8
2	CTMQC applied to the Tully Models	9
3	CTMQC applied to molecular systems	12
4	Extending surface hopping	13
4.1	Code Optimisations . . . . .	13
4.2	Electrostatics interaction within FOB-SH . . . . .	13
5	Surface hopping applied to large systems	15
6	General conclusions	16
	Appendices	17
A	Tully Model Paramters	17
A.1	Model 1 -Single Avoided Crossing . . . . .	17
A.2	Model 2 -Dual Avoided Crossing . . . . .	18
A.3	Model 3 -Extended Coupling . . . . .	18
A.4	Model 4 -Dual Arch . . . . .	19
B	Wigner Distribution Derivation	20
C	Colophon	22
	Bibliography	23

# List of Figures

2.1	Adiabatic potential energy surfaces (orange and blue) and element 1, 2 of the nonadiabatic coupling vector (black) for the 4 model systems. For parameters see appendix A. . . . .	10
-----	--	----

## List of Tables

## Chapter 1

# Introduction



## Chapter 2

# CTMQC applied to the Tully Models

The Tully models, first proposed by John Tully in 1990<sup>1</sup>, are a collection of model systems. They were designed to be simple enough to obtain accurate quantum results to benchmark new nonadiabatic molecular dynamics (NAMD) methods against. Originally there were 3, 1 dimensional, 1 atom models. However, in this work an extra model has been introduced with parameters taken from Gossel, 18<sup>2</sup>. This is to allow a full comparison of my implementation of CTMQC with the literature. In this chapter my implementation of CTMQC will be tested using these model systems and by comparing my results with those in the literature.

In each of the Tully models the (diabatic) Hamiltonian is defined by the nuclear positions and is a  $2 \times 2$  matrix that takes the form:

$$\hat{H} = \frac{\hat{p}^2}{2M} + \begin{pmatrix} H_{11}(\mathbf{R}) & H_{12}(\mathbf{R}) \\ H_{21}(\mathbf{R}) & H_{22}(\mathbf{R}) \end{pmatrix} \quad (2.1)$$

The nuclear mass is set to 2000 a.u., this was set to be very close to the proton's mass of 1836 a.u. so we can expect significant quantum effects that classical theory couldn't replicate. The values of the Hamiltonian elements are set to produce systems that resemble common features in a typical nonadiabatic simulation such as avoided crossings and regions of extended coupling. The parameters used in each systems' Hamiltonian were taken from Gossel, 18<sup>2</sup>

in order to compare the 2 implementations. These can be found in appendix A.

In order to propagate dynamics in the adiabatic basis we need to calculate various quantities from the hamiltonian at each timestep. These are, for Ehrenfest, the (adiabatic) nonadiabatic coupling vector ( $\mathbf{d}_{lk}^{(I)}$ ) and the adiabatic energies ( $E_l^{(I)}$ ). In the full CTMQC simulations we must also calculate the adiabatic momentum term  $\mathbf{f}_l^{(I)}$  from the Hamiltonian. The adiabatic energies are the eigenvalues of the Hamiltonian. The adiabatic NACV can be calculated via an (explicit Euler) finite difference method and equation (2.2) below.

$$\mathbf{d}_{lk}^{(I)} = \langle \psi_l^{(I)} | \nabla \psi_k^{(I)} \rangle \quad (2.2)$$

Where  $\psi_l^{(I)}$  is the adiabatic electronic basis function. This is given by the eigenvector of the Hamiltonian, on replica I, corresponding to state l. Illustrations of these 2 properties can be found below in fig 2.1 for each of the 4 models systems.

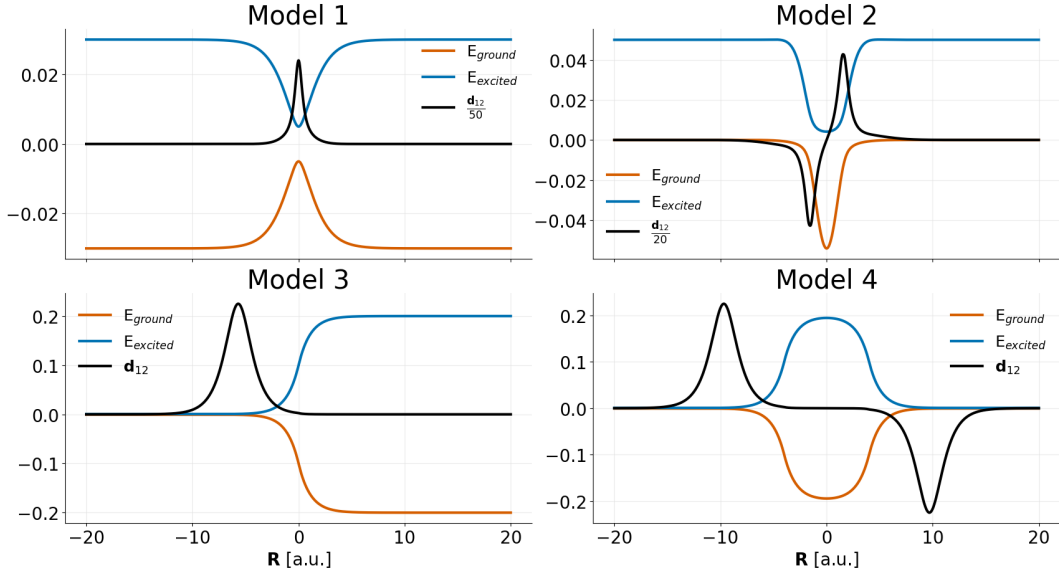


Figure 2.1: Adiabatic potential energy surfaces (orange and blue) and element 1, 2 of the nonadiabatic coupling vector (black) for the 4 model systems. For parameters see appendix A.

In order to initialise the simulations coordinates and velocities were sampled from the Wigner phase-space distribution of a gaussian nuclear wavepacket given by equation (2.3). A derivation of this can be found in appendix B.

$$\chi(R,0) = \frac{1}{(\pi\mu^2)^{\frac{1}{4}}} e^{-\frac{(R-R_0)^2}{2\mu^2} + ik_0(R-R_0)} \quad (2.3)$$

The adiabatic coefficients were initialised purely on the ground state and the initial width of the nuclear wavepacket was set to  $\mu = \sqrt{2}$  bohr. 2 values of initial momenta  $k_0$  were chosen for each model, 1 low value and another higher one. Full details of all input parameters can be found in appendix A.

## Chapter 3

# CTMQC applied to molecular systems

## Chapter 4

# Extending surface hopping

Fragment-orbital based surface hopping (FOB-SH) is a technique developed within the Blumberger group<sup>3</sup> designed to simulate large molecular systems. It has had much success in the study of organic crystalline materials<sup>4,5</sup>. Most notably the electron/hole mobilities of a variety of common organic semi-conducting materials were measured within a factor of 2 of experimental measurements. However, in order to study very large amorphous and semi-crystalline systems some more memory/computation optimisations were required and electrostatic interactions (which weren't important in previous systems) needed to be accounted for. In this chapter I outline some minor improvements I implemented within the surface hopping code as well as the method used to implement the electrostatic interactions.

### 4.1 Code Optimisations

### 4.2 Electrostatics interaction within FOB-SH

FOB-SH is a variant of Tully's original fewest switches surface hopping (ref John Tully 1990 original surface hopping paper). The electron and nuclear dynamics are dictated by the Hamiltonian, where the spatial derivative of the diagonal elements (site-energies) give the nuclear forces which come from a classical forcefield and the off-diagonal elements (electron couplings) are proportional to the overlap of the diabatic wavefunctions. Each site-energy,  $H_{\gamma\gamma}$ , is defined as the potential energy of the system where the excess charge

is localised on a single molecule,  $\gamma$ . The input parameters such as the charge distribution or the strength of the bonds are different for molecule  $\gamma$  than the other molecules, resulting in different forces/potentials. The different potentials from each permutation of the charge state are saved in the site-energies, the forces are saved in a different array of size  $(N_{states}, N_{atoms}, 3)$ .

To implement electrostatic interactions the potential and the forces within the surface hopping framework will have to be altered. In order to do this information about every permutation of charge state will have to be accounted for within the Hamiltonian.

## Chapter 5

# Surface hopping applied to large systems

## Chapter 6

## General conclusions



## Appendix A

### Tully Model Paramters

#### A.1 Model 1 -Single Avoided Crossing

	Quantity	Value	Unit
Hamiltonian Paramters:	Initial Position	-20	a.u.
	Initial Velocities	15.0, 25.0	a.u.
$H_{11}(\mathbf{R}) = A \tanh(B\mathbf{R})$	Initial Adiab Pop	ground state	-
$H_{12}(\mathbf{R}) = Ce^{-D\mathbf{R}^2}$	Simulation Time	6000, 4000	a.u.
$H_{21}(\mathbf{R}) = H_{12}(\mathbf{R})$	$\sigma_v^{(I)}$	0.5	a.u.
$H_{22}(\mathbf{R}) = -H_{11}(\mathbf{R})$	M ( $\sigma$ constant)	40	-
	$\Delta t_{\text{nuclear}}$	0.1	fs
Where A = 0.03, B = 0.4, C = 0.005	$\Delta t_{\text{electronic}}$	0.01	fs
and D = 0.3	$\frac{\delta \mathbf{R}_{lk,v}^{(I)}}{\delta t}$ threshold	0.15	a.u.
	$N_{rep}$	200	-

## A.2 Model 2 -Dual Avoided Crossing

	Quantity	Value	Unit
Hamiltonian Paramters:	Initial Position	-8	a.u.
	Initial Velocities	16.0, 30.0	a.u.
$H_{11}(\mathbf{R}) = 0$	Initial Adiab Pop	ground state	-
$H_{12}(\mathbf{R}) = Ce^{-D\mathbf{R}^2}$	Simulation Time	2500, 1500	a.u.
$H_{21}(\mathbf{R}) = H_{12}(\mathbf{R})$	$\sigma_v^{(I)}$	0.5	a.u.
$H_{22}(\mathbf{R}) = -Ae^{-B\mathbf{R}^2} + E$	M ( $\sigma$ constant)	40	-
	$\Delta t_{\text{nuclear}}$	0.1	fs
Where A = 0.1, B = 0.28, C = 0.015,	$\Delta t_{\text{electronic}}$	0.01	fs
D = 0.06 and E = 0.05	$\frac{\delta \mathbf{R}_{lk,v}^{(I)}}{\delta t}$ threshold	0.15	a.u.
	$N_{rep}$	200	-

## A.3 Model 3 -Extended Coupling

	Quantity	Value	Unit
Hamiltonian Paramters:	Initial Position	-15	a.u.
	Initial Velocities	10, 30	a.u.
$H_{11}(\mathbf{R}) = A$	Initial Adiab Pop	ground state	-
$H_{12}(\mathbf{R}) = \begin{cases} Be^{C\mathbf{R}}, & R \leq 0 \\ B(2 - e^{-C\mathbf{R}}), & R > 0 \end{cases}$	Simulation Time	5000, 1500	a.u.
$H_{21}(\mathbf{R}) = H_{12}(\mathbf{R})$	$\sigma_v^{(I)}$	0.5	a.u.
$H_{22}(\mathbf{R}) = -H_{11}(\mathbf{R})$	M ( $\sigma$ constant)	40	-
	$\Delta t_{\text{nuclear}}$	0.1	fs
	$\Delta t_{\text{electronic}}$	0.01	fs
Where A = $6 \times 10^{-4}$ , B = 0.1 and C = 0.9	$\frac{\delta \mathbf{R}_{lk,v}^{(I)}}{\delta t}$ threshold	0.15	a.u.
	$N_{rep}$	200	-

## A.4 Model 4 -Dual Arch

Hamiltonian Paramters:

$$H_{11}(\mathbf{R}) = A$$

$$H_{12}(\mathbf{R}) = \begin{cases} B \left[ -e^{C(\mathbf{R}-D)} + e^{C(\mathbf{R}+D)} \right] & R \leq -D \\ B \left[ e^{-C(\mathbf{R}-D)} - e^{-C(\mathbf{R}+D)} \right] & R \geq D \\ B \left[ 2 - e^{C(\mathbf{R}-D)} - e^{-C(\mathbf{R}+D)} \right] & -D < R < D \end{cases}$$

$$H_{21}(\mathbf{R}) = H_{12}(\mathbf{R})$$

$$H_{22}(\mathbf{R}) = -H_{11}(\mathbf{R})$$

Where  $A = 6 \times 10^{-4}$ ,  $B = 0.1$  and  $C$  $= 0.9$ 

Quantity	Value	Unit
Initial Position	-20	a.u.
Initial Velocities	10, 40	a.u.
Initial Adiab Pop	ground state	-
Simulation Time	6000, 2000	a.u.
$\sigma_v^{(I)}$	0.5	a.u.
M ( $\sigma$ constant)	40	-
$\Delta t_{\text{nuclear}}$	0.1	fs
$\Delta t_{\text{electronic}}$	0.01	fs
$\frac{\delta \mathbf{R}_{lk,v}^{(I)}}{\delta t}$ threshold	0.15	a.u.
$N_{rep}$	200	-

## Appendix B

# Wigner Distribution Derivation

The nuclear wavepacket (at time 0) is given by:

$$\chi(R) = \frac{1}{(\pi\mu^2)^{\frac{1}{4}}} e^{-\frac{(R-R_0)^2}{2\mu^2} + ik_0(R-R_0)} \quad (\text{B.1})$$

The Wigner quassiprobability function for momentum and position (p, R) is given by:

$$W(p, R) = \frac{1}{\pi\hbar} \int_{-\infty}^{\infty} \chi^*(R+y) \chi(R-y) e^{\frac{2ipy}{\hbar}} dy \quad (\text{B.2})$$

However, both Ehrenfest and CTMQC require atomic positions as input so we must extract the position and velocity probability densities from this. We get these from the marginal integrals of the Wigner distribution i.e.

$$|f(R)|^2 = \int_{-\infty}^{\infty} W(R, p) dp \quad (\text{B.3})$$

$$|f(p)|^2 = \int_{-\infty}^{\infty} W(R, p) dR \quad (\text{B.4})$$

In order to calculate these marignal integrals we must first crunch through the maths of equation (B.2). Substituting eq (B.1) into (B.2):

$$W(p, R) = \frac{1}{\pi\hbar} \int_{-\infty}^{\infty} \frac{1}{\mu\sqrt{\pi}} e^{-\frac{(R+y-R_0)^2}{2\mu^2} - 2ik_0y - \frac{(R-y-R_0)^2}{2\mu^2}} e^{\frac{2ipy}{\hbar}} dy \quad (\text{B.5})$$

Simplifying the 2 quadratic equations (equation (B.5)) we get:

$$W(p, R) = \frac{1}{\pi\hbar} \int_{-\infty}^{\infty} \frac{1}{\mu\sqrt{\pi}} e^{-\mu^{-2}(y^2 - 2ik_0 y \mu^2 + (R - R_0)^2)} e^{\frac{2ipy}{\hbar}} dy \quad (\text{B.6})$$

We can now take the expressions not dependant on y outside of the integral and combine the exponents.

$$W(p, R) = \frac{1}{\pi\sqrt{\pi}\mu\hbar} e^{-\frac{(R-R_0)^2}{\mu^2}} \int_{-\infty}^{\infty} e^{-\frac{y^2 + 2iy\mu^2(\frac{p}{\hbar} - k_0)}{\mu^2}} dy \quad (\text{B.7})$$

Integrating we get:

$$\int e^{-\frac{y^2 + 2iy\mu^2(\frac{p}{\hbar} - k_0)}{\mu^2}} dy = \frac{\sqrt{\pi}\mu}{2} e^{-\frac{\mu^2}{\hbar^2}(p - \hbar k_0)^2} \text{erf} \left[ \frac{y}{\mu} + i \left( \frac{p\mu}{\hbar} - \mu k_0 \right) \right] \quad (\text{B.8})$$

Applying limits we get:

$$\int_{-\infty}^{\infty} e^{-\frac{y^2 + 2iy\mu^2(\frac{p}{\hbar} - k_0)}{\mu^2}} dy = \sqrt{\pi}\mu e^{-\frac{\mu^2}{\hbar^2}(p - \hbar k_0)^2} \quad (\text{B.9})$$

Substituting this back into the Wigner distribution (equation (B.2)) we finally get:

$$W(p, R) = \frac{1}{\pi\hbar} e^{-\frac{(R-R_0)^2}{\mu^2}} e^{-\frac{(p - \hbar k_0)^2}{\hbar^2/\mu^2}} \quad (\text{B.10})$$

Taking the maringal integrals we get the position and velocity probability distributions:

$$|f(R)|^2 = \frac{2}{\mu\sqrt{\pi}} e^{-\frac{(R-R_0)^2}{\mu^2}} \quad (\text{B.11})$$

$$|f(p)|^2 = \frac{2}{\frac{\hbar}{\mu}\sqrt{\pi}} e^{-\frac{\mu^2}{\hbar^2}(p - \hbar k_0)^2} \quad (\text{B.12})$$

The above distributions are randomly sampled to get initial atomic velocities and positions for each simulation.

## Appendix C

# Colophon

This is a description of the tools you used to make your thesis. It helps people make future documents, reminds you, and looks good.

(example) This document was set in the Times Roman typeface using  $\text{\LaTeX}$  and  $\text{\BibTeX}$ , composed with the Atom text editor.

# Bibliography

- [1] John C. Tully. Molecular dynamics with electronic transitions. *The Journal of Chemical Physics*, 93(2):1061–1071, July 1990.
- [2] Graeme H. Gossel, Federica Agostini, and Neepta T. Maitra. Coupled-Trajectory Mixed Quantum-Classical Algorithm: A Deconstruction. *Journal of Chemical Theory and Computation*, August 2018.
- [3] J. Spencer, F. Gajdos, and J. Blumberger. FOB-SH: Fragment orbital-based surface hopping for charge carrier transport in organic and biological molecules and materials. *The Journal of Chemical Physics*, 145(6):064102, August 2016.
- [4] Samuele Giannini, Antoine Carof, and Jochen Blumberger. Crossover from Hopping to Band-Like Charge Transport in an Organic Semiconductor Model: Atomistic Nonadiabatic Molecular Dynamics Simulation. *The Journal of Physical Chemistry Letters*, 9(11):3116–3123, June 2018.
- [5] Antoine Carof, Samuele Giannini, and Jochen Blumberger. Detailed balance, internal consistency, and energy conservation in fragment orbital-based surface hopping. *The Journal of Chemical Physics*, 147(21):214113, December 2017.